Title: Influence of metastatic bone lesion type and tumor origin on human vertebral bone architecture, matrix quality, and mechanical properties

Stacyann Bailey, Ph.D. [1], Marc A. Stadelmann, Ph.D. [2], Philippe K. Zysset, Ph.D. [2], Deepak Vashishth, Ph.D. [3], and Ron N. Alkalay, Ph.D. [4 *]

[1] Department of Biomedical Engineering, University of Massachusetts Amherst, Amherst, MA.

[2] ARTORG Center for Biomedical Engineering Research, University of Bern, Freiburgstrasse 3, 3010 Bern, Switzerland

[3] Center for Biotechnology and Interdisciplinary Studies, Department of Biomedical Engineering, Rensselaer Polytechnic Institute, Troy, NY

[4] Center for Advanced Orthopedic Studies, Department of Orthopedic Surgery, Beth Israel Deaconess Medical Center and Harvard Medical School, Boston, MA.

*Address correspondence to:

Ron N. Alkalay, PhD

Associate Professor in Orthopedic Surgery

Center for Advanced Orthopedic Studies

Beth Israel Deaconess Medical Center

1 Overland Street, Boston, MA, 02215, USA

Tel.: 617-667-5185

Email: ralkalay@bidmc.harvard.edu

Short title: Metastatic lesions modulate vertebral bone properties

This article has been accepted for publication and undergone full peer review but has not been through the copyediting, typesetting, pagination and proofreading process which may lead to differences between this version and the Version of Record. Please cite this article as doi: 10.1002/jbmr.4539

Abstract

Metastatic spine disease is incurable, causing increased vertebral fracture risk and severe patient morbidity. Here, we demonstrate that osteolytic, osteosclerotic, and mixed bone metastasis uniquely modify human vertebral bone architecture and quality, affecting vertebral strength and stiffness. Multivariable analysis showed bone metastasis type dominates vertebral strength and stiffness changes, with neither age nor gender having an independent effect. In osteolytic vertebrae, bone architecture rarefaction, lower tissue mineral content and connectivity, and accumulation of advanced glycation end-products (AGEs) affected low vertebral strength and stiffness. In osteosclerotic vertebrae, high trabecular number and thickness but low AGEs, suggesting a high degree of bone remodeling, yielded high vertebral strength. Our study found that bone metastasis from prostate and breast primary cancers differentially impacted the osteosclerotic bone microenvironment, yielding altered bone architecture and accumulation of AGEs. These findings indicate that therapeutic approaches should target the restoration of bone structural integrity.

Keywords: Human vertebrae, Metastatic bone lesions, Bone architecture, Advanced Enzymatic glycation, Vertebral mechanical properties.

Introduction

Vertebral bone metastases are found in up to 70% of patients with advanced cancers [1], and for many patients, it is the first sign of malignancy [2]. Pathologic vertebral fractures (PVF) occur in 15-30% of patients with spinal bone metastasis [3] when the affected vertebra cannot withstand daily loads. Initial fracture and any subsequent vertebral collapse can lead to severe impairment of quality of life [4] and higher healthcare costs [5]. Up to 50% of the patients suffer from neurological deficits [6], leading to shortened patient survival [7] and a 3-year life expectancy [8]. With recent improvements in the survival rates of patients with primary malignancies, PVF incidence is expected to rise [9]. Identifying critical factors associated with PVF risk will improve the treatment and management of patients with metastatic spine disease.

Vertebral bone invasion with metastatic tumors is driven by cancer cell seeding, dormancy, and growth in the bone microenvironment [10], causing remarkable alterations in vertebral anatomy, vertebral bone architecture, and composition. Bone metastatic lesions are clinically classified based on radiological appearance [11]. Osteolytic bone (typical of breast, lung, urinary, and myeloma cancers) exhibits trabecular network's rarefication with a low apparent bone density and includes lytic foci of varying size (Figure 1. A). Typical of prostate and breast cancers, osteosclerotic bone (Figure. 1. B) exhibits higher apparent bone density, bone fraction, and dense trabecular network on CT imaging [12,13]. Mixed bone metastasis (typical of breast, lung, prostate cancers) [14] exhibits regions containing both the destruction of the bone network ((Figure. 1 (C_1 and C_2)) and sclerotic bone (Figure 1 (C_2)) within the vertebral anatomy. Although this subjective classification is widely used as part of the clinical management for patients at risk of vertebral fracture, it is prone to

poor agreement between clinicians [15] and is imprecise for predicting PVF risk [16]. Thus predicting PVF risk remains a significant clinical challenge [17].

This challenge partly stems from the inability of clinical imaging to fully resolve the effect of bone metastases on bone microarchitecture [18] and quality and clinical assertions regarding the effect of bone metastases on the metastatic bone's material properties. Derived from clinical observations of fracture patterns associated with the osteosclerotic and osteolytic bone metastasis [19-21], osteosclerotic bone is clinically assumed to indicate a materially stronger bone. In contrast, osteolytic bone is clinically assumed to indicate a materially weaker bone due to its radiographic appearance. At the bone tissue level, Stadelmann et al. [22] found human vertebral osteosclerotic bone to possess lower elastic modulus and ductility, while osteolytic bone demonstrated little difference in either parameter than normal bone. These findings suggest that metastatic bone architecture and material properties are complex and unique to each bone metastasis phenotype.

Bone quality (i.e., bone microarchitecture, extracellular matrix composition, mineralization, markers of bone turnover, and microdamage) is increasingly gaining interest as a contributor of bone strength independently of its mineral density [23]. Beyond bone mass, fracture susceptibility is primarily associated with aging and disease-based alterations of bone proteins, predominantly type-I collagen [24-26]. Nonenzymatic glycation (NEG), a common *in vivo* post-translational modification involving a reaction between glucose and lysine or hydroxylysine amino acid groups on type-I collagen, causes the formation of adducts known as advanced glycation end-products (AGEs). AGEs accumulation negatively affects bone fracture toughness (resistance to crack propagation)

and mechanical properties [27]. A preclinical study by Bartlow et al. [28] reported that radiation therapy increased AGEs formation in murine bone and was associated with bone embrittlement [29]. However, how bone metastasis phenotype affects AGEs accumulation in vertebral bone is unstudied and may aid in establishing new clinical modalities to reduce the risk of PVF.

This study investigated the effect of bone metastasis type on the architecture and organic matrix quality of human vertebral bone and evaluated the association between these effects and the vertebrae's strength and stiffness. We hypothesized that 1) Metastatic lesion type differentially alters both microarchitecture and accumulation of AGEs; and 2) higher AGEs accumulation, indicative of suppressed bone remodeling [30], is associated with lower vertebral strength and stiffness. For this purpose, multiple bone cores radiologically identified to contain osteolytic, osteosclerotic, and mixed bone metastasis were extracted from fourteen cadaveric vertebral bodies previously mechanically tested to measure their strength and stiffness [22]. Each bone core was μCT imaged at 10.5μm to evaluate bone microarchitecture and processed to measure the bone's collagen and AGEs content.

Materials and Methods

Figure 2 provides a graphical summary of the study's main experimental stages.

2.1 Vertebral specimens.

a. Sample Preparation: As part of a previous study [22], we obtained nine cadaver spines (3 female, 6 male, age 49-71 years, mean age 54) from donors with solid cancer (3 breast, 3 lung, 2 prostate, and 1 kidney) through the Anatomy Gifts Registry (Hanover, MD). None

of the donors had radiotherapy within 3 months before death. A standard spine imaging protocol was used to image the spines in a clinical CT scanner (Aquilion 64, Toshiba Medical, USA) [22] with forty-five vertebral segments demonstrating osteolytic, osteosclerotic, or mixed bone metastasis extracted based on radiological review.

b. Mechanical Testing [22]: In brief, each vertebral level was prepared to obtain plano-parallel vertebral body sections, 12mm to 25mm in height, and the vertebral segments imaged at 24.5 μm isotropic voxel size (μCT100, Scanco Medical, Bruettisellen) [22]. Based on our laboratory protocol [31], bone tissue was segmented, and the vertebral center of mass (COM) was computed [32] to standardize the mechanical testing loading point.

Each vertebral segment was equilibrated in a 0.9% NaCl saline solution (one hour at room temperature) [32], followed by a test to failure under monotonic (5 mm/min) axial compressive displacement [22]. With the test completed, the vertebral segment was wrapped in saline-soaked gauze and stored at − 20 °C in double plastic bags to await bone coring. Vertebral strength was defined as the maximum compressive force measured from the load-displacement curve. Vertebral stiffness was computed from a linear regression model's coefficient fitted to the linear portion of the load-displacement curve (10 - 90% of the maximum compressive force). Segment's demographics, bone mineral content values, strength, and structural stiffness values are summarized in Table 1 (Appendix). Based on the mechanical tests, fourteen vertebrae demonstrating either maximum or minimum strength values were selected to retrieve bone core samples.

2.2 Bone core samples.

a. Selection and Preparation: For each selected vertebrae, the axial and sagittal vertebral μCT images [22] were reviewed and, based on the bone radiological appearance, 4-6

locations in the body cross-section showing either osteolytic, osteosclerotic, mixed bone metastasis, or no radiological evidence of bone metastasis, were selected for bone core retrieval. Each core image-based X, Y coordinates were computed, and the core was extracted under constant water irrigation using a diamond-coated coring drill (5.08mm inner diameter, model 102055, Starlite industries, Rosemont, PA, USA) mounted on a CNC milling device. Each core was tagged, wrapped in saline-soaked gauze, and stored at − 20 °C in 1.5mL microtubes (MaxyClear, Fisher scientific, USA).

b. Bone core imaging: The bone cores were immersed in saline using a custom imaging chamber and μCT imaged at 10.5μm voxel size (vivaCT 40; 70 kVp, 114mA, and 200ms integration time, Scanco Medical AG, Bassersdorf, Switzerland). Each core was re-tagged, wrapped in saline-soaked gauze, and stored in 1.5mL microtubes (Axygen™ MaxyClear, Fisher scientific, USA) at − 20 °C. Based on the radiological review of the μCT image data, each bone core was assigned a bone metastasis type (Appendix, Table A.1). A threshold value of 419 mgHA/cm^3 was used for bone segmentation, and the μCT analysis software was used to compute the following bone architectural parameters: bone volume fraction, BV/TV (%), trabecular number, TbN (1/mm), trabecular thickness, TbTh (mm), trabecular separation, TbSp (mm), and connectivity density, ConnD (1/mm3). Bone mineral content, BMC (mgHA), was computed from the complete bone core volume segmentation.

c. Measurement of the bone core total Fluorescent Advanced Glycation End-products: Each imaged core was thawed, sectioned transversely to obtain two small cylindrical specimens (15-20 mm length x 5 mm diameter, ~40-50mg dry weight). The prepared bone specimens were defatted using isopropyl ether, lyophilized (freeze-dried) overnight, and

hydrolyzed in 6N hydrochloric acid (HCL) based on dry weight for 16 hours. Fluorescence was measured for quinine sulfate standard (stock: 10μg/mL quinine per 0.1N sulfuric acid) and hydrolysate from the individual bone specimens at 360/460 excitation/emission [33] using an Infinite 200 microplate reader (Tecan, Männedorf, Switzerland). The sample's collagen content was calculated using a hydroxyproline standard of increasing concentration (stock: 2000 μg/mL L-hydroxyproline per 0.001 N HCL) [33]. The absorbance of the hydrolysates and hydroxyproline standard were subsequently measured at 570nm. Total fluorescent AGEs were computed as the amount of quinine per unit of collagen [33] with fluorescence and absorbance measured using the microplate reader (Infinite 200, Tecan).

2.3 Statistical Analysis.

Statistical analyses were performed in JMP Pro (V14.3, SAS Institute, Inc., NC). Univariate analysis was applied to test for normality of distribution for bone architectural properties, BMC, AGEs, and collagen. Based on this analysis, we applied Kruskal–Wallis one-way ANOVA to test for the effect of bone metastasis phenotype (the independent variable) on; 1) vertebral strength, 2) vertebral stiffness, 3) imaged derived bone architectural parameters: (BMC, BV/TV, TbN, TbTh, TbSp, and ConnD) and 4) measured AGEs and collagen content. Dunn With Control for Joint Ranks was used for post-hoc testing [34].

The sampling of multiple vertebrae per spine can introduce clustering (non-independence) of the data [35]. We fitted linear mixed-effects models (LMM) under different assumptions about the correlation structure among segments from the same spines to test this effect on the association of BMC, AGEs, and collagen with the bone architectural parameters. Based

on the corrected Akaike information criterion (AICc), the independence structure best fits the data [35] (i.e., a lack of correlation among segments from the same spine).

With multiple cores obtained per vertebra, we applied multivariable LMM regression to test the independent contribution of the bone core's 1) age, 2) gender, 3) race, 4) BV/TV, 6) architectural parameters, and 7) AGEs and Collagen content to the vertebral bodies measured strength and structural stiffness. Given that the strength of three vertebrae was greater than the limits of the testing system (15kN), the true strength of these vertebrae was not ascertained (right-censored data). We repeated the multivariable model for the strength analysis using tobin regression (allowing for a censored observed range of the dependent variable, which, in this case, was vertebral strength>15kN). Based on AICc, we found the LMM model best fitted the association between the bone core data and the vertebral strength and stiffness. The LMM analyses were repeated for each bone metastasis type to test whether the model's prediction for vertebral strength and stiffness was retained for individual bone metastasis types. Statistical significance was set at the 5% level.

Results

3.1 Metastatic bone type alters vertebral strength and stiffness.

ANOVA analysis found that bone metastasis phenotype significantly affects vertebral strength ($p=0.0078$) and stiffness ($p=0.0208$). Post-hoc analysis showed osteosclerotic vertebrae with higher strength ($p=0.0049$) and stiffness ($p=0.0264$) than osteolytic vertebrae, Figure 3.

3.2 Bone metastases type modulates bone mineral content and architecture.

Univariate statistics revealed bone tissue mineral content and architectural indices to be non-normally distributed. Compared to mixed and osteolytic bone metastases, osteosclerotic bone showed higher BMC values (72%, p=0.0049, and 257%, p<0.0001), TbN (34%, p=0.0023, and 69%, p<0.0001) and TbTh (35%, p=0.0196 and 52.4%, p=0.0003) but with lower TbSp (60%, p=0.0003 and 68%, p<0.0001), Figure 4. These differences manifested in higher ConnD (63%, p=0.0023 and 93%, p<0.0001) and BV/TV (57%, p=0.0010, and 76%, p<0.0001). Bone with mixed bone metastasis had higher BMC (108%, p<0.0001), BV/TV (82%, p<0.0001), TbN (54%, p<0.0001), ConnD (83%, p=0.0005) but lower TbSp (-96%, p<0.0001) than osteolytic bone, Figure 4. Our analysis further revel that osteosclerotic bone from breast cancer donors exhibted higher ConnD, a median (Q1-Q3) of 133.6 (77.3-194.7) than osteosclerotic bone from prostate cancer donors,60.0 (44.0-70.2), the diffenrce ststiaclly significnat (p=0.0145), Figure 5.

3.3 Bone metastases type differentially affect the association of bone volume fraction with bone architecture.

We found distinct associations between the phenotype of bone metastasis and alterations in the vertebral bone BV/TV, BMC, and architectural indices (Figure 6):

- Osteolytic bone: BV/TV was associated with higher BMC (R^2=0.86, p<0.0001), TbN (R^2=0.74, p<0.0001) and ConnD (R^2=0.47, p<0.0001) and with lower TbSp (R^2=0.61, p<0.0001). BV/TV was not significantly associated with TbTh (R^2=0.01, p=0.6427).
- Osteosclerotic bone: BV/TV was associated with higher BMC (R^2=0.42, p<0.0001), TbTh (R^2=0.69, p=0.0003), TbN (R^2=0.31, p=0.0370) and with lower TbSp (R^2=0.51 ,p=0.0043). However, BV/TV and ConnD was not significantly associated, Figure 6.

- Mixed BM bone: Similar to the osteosclerotic bone, BV/TV was associated with higher BMC (R^2=0.80, p=0.0004) and TbTh (R^2=0.84, p=0.0002). Similar to the osteolytic bone, BV/TV was associated with higher ConnD (R^2=0.64, p=0.0055). BV/TV was not significantly associated with TbSp or TbN (Figure 6).

Multivariable analysis, used to investigate the independent contribution of BMC, architecture (TbN, TbSp, TbTh, ConnD) and age, to BV/TV, found distinct differences between the BM phenotypes. In osteolytic bone, the model explained 88% of the variation in BV/TV (F:72.11, p<0.0001) with TbSp (p<0.0001), TbTh (p<0.0001) and ConnD (p=0.0005) as significant independent correlates of BV/TV. In osteosclerotic bone, the model explained 94% of the variation in BV/TV (F:72.08, p<0.0001) with TbSp (p<0.0001) and TbTh (p<0.0001) significant independent correlates of BV/TV. In mixed bone metastasis, the model explained 98% of the variation in BV/TV (F: 73. 01, p=0.0024) with TbTh (p=0.0001) and TbN (p=0.0405) significant independent correlates of BV/TV.

3.4 Accumulation of advanced glycation end-products (AGEs) is lesion type dependent.

We measured the amount of collagen and the modification of collagen by nonenzymatic crosslinking (by the accumulation of AGEs) to gain insight into the modification of bone matrix, particularly proteins, and identify matrix-based mechanisms contributing to the altered bone structural organization and mechanics. Bone metastasis phenotype significantly affected both AGEs accumulation (p=0.0004) and collagen content (p=0.0003) in the bone samples (Figure 7). Post-hoc comparisons showed osteosclerotic bone to exhibit significantly lower AGEs and higher collagen content compared to the osteolytic (a median difference of -159.4% (p=0.0012) and 60.8%, p<0.0001 respectively)

and mixed bone metastases (-226.7%, p=0.0002 and 185.5%, p=0.0002), Figure 7. There was no statistically significant difference between mixed bone metastasis and osteolytic bone for AGEs or collagen content. Independent of bone metastasis type, LMM analysis found AGEs correlated with higher TbSp (F=8.7, p=0.0049) and lower BMC (f=8.44, p=0.0054), and TbN (F=11.0, p=0.0016). Of note, we observed no significant correlation for AGEs with TbTh. No significant correlation was found between collagen content and the bone architecture indices.

3.5 BMC, AGEs, and bone architecture affect metastatic vertebral strength and stiffness.

LMM analysis showed that multiple sampling of bone cores per vertebrae had no significant effect on these associations (Wald p test >0.05). Univariate LMM analysis of the pooled data (independent of bone metastasis phenotype) revealed a higher BMC and lower AGEs associated with higher vertebral strength (F=37.38, p<0.0001 and, F=12.72, p=0.0020) and stiffness (F=18.72, p<0.0001, and F=6.02, p=0.0206), Figure 8. For bone architectural parameters, higher vertebral strength was associated with higher TbN (F=60.44, p<0.0001), ConnD (F=54.75, p<0.0001), TbTh (F=4.55, p=0.0380), and lower TbSp (F=35.16, p<0.0001). Vertebral stiffness was associated with higher TbN (F=30.48, p<0.0001) and ConnD (F=35.57, p<0.0001) but lower TbSp (F=15.65, p=0.0001).

Multivariate LMM analysis, incorporating age, gender, BV/TV, BMC, architectural indices, and AGEs (modeled as fixed effects) with vertebral level set as a random variable, showed age (p=0.0012), Tb.Sp (p<0.0001) and ConnD (p<0.0001) to be significant independent correlates of the measured vertebral strength. BV/TV was a

significant independent correlate (p=0.0112) of vertebral stiffness with Tb.Th at near significance as an independent correlate (p=0.0707).

Discussion

This study demonstrated that osteosclerotic, osteolytic, and mixed bone metastases uniquely alter BMC and the architectural features of cadaveric vertebral cancellous bone from donors with a range of solid sarcomas. Bone metastases types were associated with distinct differences in the accumulation of AGEs within the organic bone matrix, suggesting that lesions influence bone cellular activity/turnover and, consequently, bone matrix nanoindentation properties [22]. Gender also affected distinct differences in microarchitecture and AGEs accumulation in osteosclerotic but not osteolytic bone.

Preclinical murine models of osteolytic and mixed skeletal metastases [36-38] attributed the decrease in bone fraction to the significant but incomplete loss of physical trabeculae, i.e., a lower number and thinner bone trabeculae with reduced bone connectivity [38,39]. Consistent with these reports, we found that a lower number of bone trabeculae with reduced connectivity, older age, and female gender were associated with greater BMC and BV/TV loss in human osteolytic vertebral bone. In contrast to preclinical models [38,39], we did not observe an association between changes in trabecular thickness and BV/TV in the human bone samples. However, our study's strong association between lower bone connectivity and lower bone fraction suggests that osteolytic lesions affect bone loss in human bone by eliminating rather than thinning the bone trabeculae. Furthermore, we found that osteolytic bone tissue contained higher AGEs, suggesting that osteolytic bone

exhibited limited new bone tissue formation and contained older and more fragile bone tissue [27]. The accumulation of AGEs is reported to be associated with reduced bone formation [40], caused by reduced osteoblastic differentiation and activity [41], and reduced bone resorption, caused by reduced osteoclastic activity [42]. Our finding of more rods than plates in the osteolytic case is consistent with previous studies that showed AGEs are higher in trabecular rods than plates that are preferentially lost with age [33].

In contrast to osteolytic, osteosclerotic bone regions were radiologically characterized by high BMC and BV/TV [11]. In human bone from prostate cancer patients, osteosclerotic bone exhibits an increased number of bone trabeculae and bone surface area and a lower degree of structural anisotropy than healthy bone [12,13]. Consistent with these reports, our stereological analysis showed trabecular thickening and decreased intertrabecular distance with higher BMC in the osteosclerotic bone (up to 30% of samples had BV/TV values > 50%, suggesting a near-solid bone). However, in contrast to studies in human [12,13] and mouse [39] osteosclerotic vertebral bone, neither new bone trabeculae nor higher bone connectivity was associated with higher BMC. Indeed, similar to previously reported histological observation of unorganized woven structure in newly remodeled osteosclerotic bone [43], and in concert with trabecular thickening and higher BV/TV, we found the osteosclerotic bone to contain more collagen and exhibit lower AGEs values indicative of increased matrix production in the newly deposited osteoid-like mineralized bone tissue. These findings suggest that increased BMC occurs via extensive bone deposition and remodeling of the existing bone trabeculae network.

This study found differences in the bone architecture of osteosclerotic bone obtained from breast and prostate cancer donors. In osteosclerotic bone obtained from

breast cancer donors, we observed an abundant deposition of mineralized bone-like tissue in the marrow spaces, increased number of bone trabeculae, and lower intertrabecular spacing with little evidence of trabecular thickening. In contrast, osteosclerotic bone obtained from prostate cancer showed opposite micro-architectural features. Endocrine [44] and paracrine [45] factors modulate the interaction of breast and prostate cancer-derived metastatic tumor cells, including the differentiation, proliferation, and maturation of osteoblasts and the inhibition of osteoclasts [46], resulting in uncontrolled bone formation [47]. Although the mechanism underlying the observed differences in osteosclerotic bone architecture is unknown, this novel finding suggests that primary cancer (breast vs. prostate) may result in distinct differences in micro-architectural features of the osteosclerotic bone tissue. Whether these differences affect, the osteosclerotic vertebral bone failure process is under active investigation in our laboratory.

Preclinical studies reported bone with mixed bone metastasis to exhibit increased osteolysis, indicated by increased osteoclast number and decreased bone volume with regions of enhanced yet immature bone growth [38]. Furthermore, in canine models of prostate cancer, lesions yielding mixed bone metastasis exhibited lower trabecular number and spacing (generalized loss of trabecular bone rather than trabecular thickness) [48]. In agreement with these reports, this study's stereological analysis found that human bone with mixed bone metastasis exhibited features typical of osteosclerotic (higher bone trabecular thickness associated with higher BMC) and osteolytic (moderate association of BMC with ConnD) bone. However, in these cases, BMC was weakly associated with either trabecular number or separation compared to osteolytic or osteosclerotic bone tissues. Although research on the effect of mixed bone metastasis on human bone microarchitecture

is rare, our findings in humans and the previous finding of murine models [38] suggest that incomplete osteosclerotic activity rather than excessive resorption dominate the structural changes in bone with mixed bone metastasis.

We found that AGEs normalized to bone collagen were significantly higher in bone with osteolytic and mixed bone metastasis than with osteosclerotic bone metastasis. Newly formed and younger bone matrix contains lower AGEs [49]. The presence of lower AGEs in osteosclerotic bone metastasis is likely to result from increased collagen production (See Figure 5), present in newly formed osteoid-like mineralized bone. In contrast, osteolytic, mixed bone metastasis, and older trabeculae are higher in AGEs [33]. Our results agree with previous studies demonstrating an increase in AGEs, namely pentoside (PEN) and carboxymethylysine (CML), with osteolytic involvement [50,51]. Here, we measured total fluorescent AGEs in bulk, including PEN, to highlight the role of sugar-induced AGEs in osteolytic and mixed bone metastasis for the first time. Our finding of high AGEs in osteolytic bone tissue compared to the mixed and osteosclerotic bone tissue suggests reduced bone formation leaving behind older bone tissue [33]. Thus, the accumulation of AGEs may also modify cell-matrix interactions altering subsequent osteoblastic and osteoclastic differentiation, influencing bone architecture and mechanical properties, and contributing to the differences observed between osteolytic and osteosclerotic bone.

Vertebral cancellous bone, representing a foam-based structure designed to achieve high strength and stiffness with relatively small mass amounts, forms the predominant load-carrying structure in the vertebral body [52]. Studies in mouse [39] and human [53] bone samples highlighted BMC, BV/TV, and specific architectural features (higher trabecular thickness and lower inter-trabecular spacing) as determinants of metastatic bone strength.

Although we tested a limited number of human vertebral specimens demonstrating a range of bone metastasis types, we found that metastatic lesion's effect on bone mineral content and architectural features was strongly associated with vertebral strength and stiffness. Previous findings demonstrated that metastatically involved bone experienced higher strains localized to areas of degraded osteolytic bone [54]. In our study, severely disrupted structural synergism between bone stereology (trabecular separation, number, and connectivity) and the tissue mineral content suggests that this altered structural loading may affect early failure initiation and loss of vertebral strength.

The contribution of bone "quality" to pathologic bone strength remains unclear. The accumulation of AGEs in aged bone tissue is linked with altered architecture (higher in rods than plates [33] and reduced toughness [55,56], which in turn reduces bone resistance to fracture. Consistent with these studies, we found higher bone AGEs accumulation associated with lower vertebral strength. However, the osteosclerotic bone showed high BMC, more collagen, and low AGEs accumulation. Such differences indicate that osteosclerotic bone tissue is different from osteolytic bone tissue and may consist of newly deposited and less mineralized woven bone [57] that exhibits slightly lower mean indentation modulus [22,50] mean hardness [50], and ductility [22]. Indeed, our stereology analysis suggests the osteosclerotic vertebrae's high strength and stiffness are achieved by the abundant deposition of new bone material rather than improved bone structural network and bone material properties. Consistent with Burke et al. [39], our observations indicate that metastatic lesions change bone mineral content, structure and composition to affect vertebral mechanical behavior.

Our study has several limitations. Cancer patients are exposed to extensive oncological treatments, including chemotherapy, immunotherapy, and radiotherapy, affecting bone architecture and density and, consequently, vertebral fracture risk [58,59]. Although we had the donor's medical history, primary cancer diagnosis, chemotherapy, pharmacological, and surgical treatments, we had little information regarding radiotherapy and, if so, which levels were treated. Hence, we cannot discount that these treatments could have affected the measured vertebral bodies' strength and stiffness and collagen and AGEs values. The fourteen vertebral bodies employed in this study were from nine donors with a range of primary cancers and were exposed to mechanical testing as part of a previous study. Our bone cores were selected from these mechanically tested vertebral bodies. Although the micro-CT images did not reveal the bone architecture to be damaged, we cannot assume that the previous testing did not impose mechanical damage at the bone tissue level.

Given that in cortical bone, both magnitude and the type of damage affected indentation derived material parameters and other mechanical properties of [60], we did not measure the bone cores' strength and stiffness. Our previous work demonstrated whole vertebral BMC and the computation of vertebral strength based on homogenised finite element analysis to provide moderate [BMC: R^2=0.66, $p<0.001$] and strong [hFE: R^2=0.78, $p<0.001$] prediction of pathologic vertebral strength [22], suggesting that the mechanical properties of the pathologic vertebral body are driven predominantly by spatial distribution and densitometric properties of the lesioned bone. This study finding of the association between bone metastasis's type and change in bone architectural indices and AGEs suggests that additional work is needed to understand better whether the effect of metastasis on bone quality significantly contributes to the strength of whole human pathologic vertebrae.

In conclusion, metastatic tumors affect human vertebral bodies by altering bone mineral content, microarchitecture, and extracellular matrix composition. Primary cancers vary significantly within lesion types, particularly for osteolytic bone metastasis. Each lesion type also confers a distinct alteration of bone structure and, to a lesser extent, material properties independently of the primary tumor origin. Therapeutic approaches should, therefore, target the restoration of bone structural integrity. The relationships highlighted in this study may aid in forming the foundation for technologies to assess the risk of pathologic fracture clinically.

Acknowledgments

This study was supported by the National Institute of Arthritis and Musculoskeletal and Skin Diseases grant (AR055582), the Center for Biotechnology and Interdisciplinary Studies (CBIS) BioImaging Core Preliminary Studies Award, and by the Rensselaer Polytechnic Institute Van Auken Postdoctoral Fellowship. Marc Stadelmann was supported by grant no 147153 of the Swiss National Science Foundation (SNSF).

Data Availability Statement: The data that support the findings of this study are available on request from the corresponding author. The data are not publicly available due to privacy or ethical restrictions.

References

1. Siegel R, DeSantis C, Virgo K, Stein K, Mariotto A, Smith T, et al. Cancer treatment and survivorship statistics, 2012. CA Cancer J Clin. 2012;62(4):220-41.
2. Schiff D, O'Neill BP, Suman VJ. Spinal epidural metastasis as the initial manifestation of malignancy: clinical features and diagnostic approach. Neurology. 1997;49(2):452-6.
3. Prasad D, Schiff D. Malignant spinal-cord compression. Lancet Oncol. 2005;6(1):15 - 24.
4. Pond GR, Sonpavde G, de Wit R, Eisenberger MA, Tannock IF, Armstrong AJ. The prognostic importance of metastatic site in men with metastatic castration-resistant prostate cancer. Eur Urol. Jan 2014;65(1):3-6.
5. Barlev A, Pharm D, Song X, Ivanov B, Setty V, Karen C, et al. Payer Costs for Inpatient Treatment of Pathologic Fracture, Surgery to Bone, and Spinal Cord Compression Among Patients with Multiple Myeloma or Bone Metastasis Secondary to Prostate or Breast Cancer. J Manag Care Pharm. 2010 16(9):693-702.
6. Walls J, Bundred N, Howell A. Hypercalcemia and bone resorption in malignancy. Clin Orthop. 1995;312(51):51-63.
7. Saad F, Lipton A, Cook R, Chen YM, Smith M, Coleman R. Pathologic fractures correlate with reduced survival in patients with malignant bone disease. Cancer. 2007;110(8):1860-7.
8. Oefelein MG, Conrad VR, Resnick MI. Skeletal fractures negatively correlate with overall survival in men with prostate cancer. J Urol. 2002;168(3):1005-7.

9. Bollen L, Jacobs WCH, Van der Linden YM, Van der Hel O, Taal W, Dijkstra PDS. A systematic review of prognostic factors predicting survival in patients with spinal bone metastases. Eur Spine J. Apr 2018;27(4):799-805.

10. Fornetti J, Welm AL, Stewart SA. Understanding the Bone in Cancer Metastasis. J Bone Miner Res. Dec 2018;33(12):2099-113.

11. Guise TA, Mohammad KS, Clines G, Stebbins EG, Wong DH, Higgins LS, et al. Basic mechanisms responsible for osteolytic and osteoblastic bone metastases. Clin Cancer Res. Oct 15 2006;12(20 Pt 2):6213s-6s.

12. Sone T, Tamada T, Jo Y, Miyoshi H, Fukunaga M. Analysis of three-dimensional microarchitecture and degree of mineralization in bone metastases from prostate cancer using synchrotron microcomputed tomography. Bone. Aug 2004;35(2):432-8.

13. Tamada T, Sone T, Jo Y, Imai S, Kajihara Y, Fukunaga M. Three-dimensional trabecular bone architecture of the lumbar spine in bone metastasis from prostate cancer: comparison with degenerative sclerosis. Skeletal Radiol. 2005;34(3):149-55.

14. Mundy GR. Metastasis to bone: causes, consequences and therapeutic opportunities. Nat Rev Cancer. Aug 2002;2(8):584-93.

15. Fourney DR, Frangou EM, Ryken TC, Dipaola CP, Shaffrey CI, Berven SH, et al. Spinal instability neoplastic score: an analysis of reliability and validity from the spine oncology study group. J Clin Oncol. 2011;29(22):3072-7.

16. Sung SH, Chang UK. Evaluation of risk factors for vertebral compression fracture after stereotactic radiosurgery in spinal tumor patients. Korean J Spine. 2014;11(2):103-8.

17. Weber MH, Burch S, Buckley J, Schmidt MH, Fehlings MG, Vrionis FD, et al. Instability and impending instability of the thoracolumbar spine in patients with spinal metastases: a systematic review. Int J Oncol. 2011;38(11):5-12.

18. Tabor Z. Analysis of the influence of image resolution on the discriminating power of trabecular bone architectural parameters. Bone. Jan 2004;34(1):170-9. Epub 2004/01/31.

19. Borggrefe J, Giravent S, Campbell G, Thomsen F, Chang D, Franke M, et al. Association of osteolytic lesions, bone mineral loss and trabecular sclerosis with prevalent vertebral fractures in patients with multiple myeloma. Eur J Radiol. 2015;84(11):2269-74.

20. Greenspan SL, Wagner J, Nelson JB, Perera S, Britton C, Resnick NM. Vertebral fractures and trabecular microstructure in men with prostate cancer on androgen deprivation therapy. J Bone Miner Res. Feb 2013;28(2):325-32.

21. Lad SP, Patil CG, Lad EM, Boakye M. Trends in pathological vertebral fractures in the United States:1993 to 2004. J Neurosurg Spine. 2007;7(3):305-10.

22. Stadelmann MA, Schenk DE, Maquer G, Lenherr C, Buck FM, Bosshardt DD, et al. Conventional finite element models estimate the strength of metastatic human vertebrae despite alterations of the bone's tissue and structure. Bone. 2020;141:115598.

23. Felsenberg D, Boonen S. The bone quality framework: determinants of bone strength and their interrelationships, and implications for osteoporosis management. Clin Ther. Jan 2005;27(1):1-11.

24. Bailey AJ, Paul RG, Knott L. Mechanisms of maturation and ageing of collagen. Mech Ageing Dev. Dec 1 1998;106(1-2):1-56.

25. Wang X, Shen X, Li X, Agrawal CM. Age-related changes in the collagen network and toughness of bone. Bone. Jul 2002;31(1):1-7.

26. Boskey AL, Spevak L, Weinstein RS. Spectroscopic markers of bone quality in alendronate-treated postmenopausal women. Osteoporos Int. May 2009;20(5):793-800.

27. Vashishth D. Advanced Glycation End-products and Bone Fractures. IBMS Bonekey. Aug 2009;6(8):268-78.

28. Bartlow CM, Mann KA, Damron TA, Oest ME. Limited field radiation therapy results in decreased bone fracture toughness in a murine model. PLoS One. 2018;13(10):e0204928.

29. Mandair GS, Oest ME, Mann KA, Morris MD, Damron TA, Kohn DH. Radiation-induced changes to bone composition extend beyond periosteal bone. Bone Rep. Jun 2020;12:100262.

30. Tang SY, Allen MR, Phipps R, Burr DB, Vashishth D. Changes in non-enzymatic glycation and its association with altered mechanical properties following 1-year treatment with risedronate or alendronate. Osteoporos Int. Jun 2009;20(6):887-94. Epub 2008/10/14.

31. Burghardt AJ, Kazakia GJ, Majumdar S. A local adaptive threshold strategy for high resolution peripheral quantitative computed tomography of trabecular bone. Annals of Biomedical Engineering. 2007;35(10):1678-86.

32. Dall'Ara E, Schmidt R, Pahr D, Varga P, Chevalier Y, Patsch J, et al. A nonlinear finite element model validation study based on a novel experimental technique for inducing anterior wedge-shape fractures in human vertebral bodies in vitro. J Biomech. Aug 26 2010;43(12):2374-80.

33. Karim L, Vashishth D. Heterogeneous glycation of cancellous bone and its association with bone quality and fragility. PLoS One. 2012;7(4):e35047.

34. Riffenburgh RH. Statistics in Medicine. 3rd ed. San Diego, CA: Elsevler's Academic Press; 2012.

35. O'Brien L, Fitzmaurice G. Analysis of longitudinal multiple source binary data using generalized estimating equations. . Appl Statist. 2004;53(1):177-93.

36. Bi X, Sterling JA, Merkel AR, Perrien DS, Nyman JS, Mahadevan-Jansen A. Prostate cancer metastases alter bone mineral and matrix composition independent of effects on bone architecture in mice--a quantitative study using microCT and Raman spectroscopy. Bone. Oct 2013;56(2):454-60.

37. Kurth AA, Muller R. The effect of an osteolytic tumor on the three-dimensional trabecular bone morphology in an animal model. Skeletal Radiol. Feb 2001;30(2):94-8.

38. Wise-Milestone L, Akens MK, Rosol TJ, Hojjat SP, Grynpas MD, Whyne CM. Evaluating the effects of mixed osteolytic/osteoblastic metastasis on vertebral bone quality in a new rat model. J Orthop Res. May 2012;30(5):817-23.

39. Burke M, Akens M, Kiss A, Willett T, Whyne C. Mechanical behavior of metastatic vertebrae are influenced by tissue architecture, mineral content, and organic feature alterations. J Orthop Res. Nov 2018;36(11):3013-22. Epub 2018/07/07.

40. Yang X, Mostafa AJ, Appleford M, Sun LW, Wang X. Bone Formation is Affected by Matrix Advanced Glycation End Products (AGEs) In Vivo. Calcif Tissue Int. Oct 2016;99(4):373-83. Epub 2016/06/01.

41. Kume S, Kato S, Yamagishi S, Inagaki Y, Ueda S, Arima N, et al. Advanced glycation end-products attenuate human mesenchymal stem cells and prevent cognate differentiation into adipose tissue, cartilage, and bone. J Bone Miner Res. Sep 2005;20(9):1647-58. Epub 2005/08/02.

42. Valcourt U, Merle B, Gineyts E, Viguet-Carrin S, Delmas PD, Garnero P. Non-enzymatic glycation of bone collagen modifies osteoclastic activity and differentiation. J Biol Chem. Feb 23 2007;282(8):5691-703. Epub 2006/12/05.

43. Roudier MP, Vesselle H, True LD, Higano CS, Ott SM, King SH, et al. Bone histology at autopsy and matched bone scintigraphy findings in patients with hormone refractory prostate cancer: the effect of bisphosphonate therapy on bone scintigraphy results. Clin Exp Metastasis. 2003;20(2):171-80. Epub 2003/04/23.

44. Mishra S, Tai Q, Gu X, Schmitz J, Poullard A, Fajardo RJ, et al. Estrogen and estrogen receptor alpha promotes malignancy and osteoblastic tumorigenesis in prostate cancer. Oncotarget. Dec 29 2015;6(42):44388-402. Epub 2015/11/18.

45. Ren G, Esposito M, Kang Y. Bone metastasis and the metastatic niche. J Mol Med (Berl). Nov 2015;93(11):1203-12.

46. Hofbauer LC, Rachner TD, Coleman RE, Jakob F. Endocrine aspects of bone metastases. Lancet Diabetes Endocrinol. Jun 2014;2(6):500-12. Epub 2014/06/02.

47. Battafarano G, Rossi M, Marampon F, Del Fattore A. Cellular and Molecular Mediators of Bone Metastatic Lesions. Int J Mol Sci. Jun 8 2018;19(6). Epub 2018/06/13.

48. LeRoy BE, Thudi NK, Nadella MV, Toribio RE, Tannehill-Gregg SH, van Bokhoven A, et al. New bone formation and osteolysis by a metastatic, highly invasive canine prostate carcinoma xenograft. Prostate. Aug 1 2006;66(11):1213-22.

49. Sroga GE, Karim L, Colon W, Vashishth D. Biochemical characterization of major bone-matrix proteins using nanoscale-size bone samples and proteomics methodology. Mol Cell Proteomics. Sep 2011;10(9):M110 006718. Epub 2011/05/25.

50. Burke MV, Atkins A, Akens M, Willett TL, Whyne CM. Osteolytic and mixed cancer metastasis modulates collagen and mineral parameters within rat vertebral bone matrix. J Orthop Res. Dec 2016;34(12):2126-36.

51. Nass N, Ignatov A, Andreas L, Weissenborn C, Kalinski T, Sel S. Accumulation of the advanced glycation end product carboxymethyl lysine in breast cancer is positively associated with estrogen receptor expression and unfavorable prognosis in estrogen receptor-negative cases. Histochem Cell Biol. May 2017;147(5):625-34.

52. Keaveny TM, Hayes WC. A 20-year perspective on the mechanical properties of trabecular bone. J Biomech Eng. 1993;115:534 -42.

53. Nazarian A, Stechow DV, Zurakowski D, Müller R, Snyder BD. Bone volume fraction explains the variation in strength and stiffness of cancellous bone affected by metastatic cancer and osteoporosis. Calcif Tissue Int. 2008;83(6):368-79.

54. Hardisty MR, Akens MK, Hojjat SP, Yee A, Whyne CM. Quantification of the effect of osteolytic metastases on bone strain within whole vertebrae using image registration. J Orthop Res. 2012;30(7):1032-9.

55. Vashishth D, Gibson GJ, Khoury JI, Schaffler MB, Kimura J, Fyhrie DP. Influence of nonenzymatic glycation on biomechanical properties of cortical bone. Bone. Feb 2001;28(2):195-201. Epub 2001/02/22.

56. Zimmermann EA, Schaible E, Bale H, Barth HD, Tang SY, Reichert P, et al. Age-related changes in the plasticity and toughness of human cortical bone at multiple length scales. Proc Natl Acad Sci U S A. Aug 30 2011;108(35):14416-21. Epub 2011/08/30.

57. Burke M, Atkins A, Kiss A, Akens M, Yee A, Whyne C. The impact of metastasis on the mineral phase of vertebral bone tissue. J Mech Behav Biomed Mater. May 2017;69:75-84.

58. Cunha MV, Al-Omair A, Atenafu EG, Masucci GL, Letourneau D, Korol R, et al. Vertebral compression fracture (VCF) after spine stereotactic body radiation therapy (SBRT): analysis of predictive factors. Int J Radiat Oncol Biol Phys. Nov 1 2012;84(3):e343-9.

59. Guise TA. Bone loss and fracture risk associated with cancer therapy. Oncologist 2006;11(10):1121-31.

60. Diab T, Sit S, Kim D, Rho J, Vashishth D. Age-dependent fatigue behaviour of human cortical bone. Eur J Morphol. Feb-Apr 2005;42(1-2):53-9. Epub 2005/08/27.

Figure 1. Sagittal and axial images of whole human vertebral specimens with osteolytic, osteosclerotic, and mixed bone metastasis with regions demonstrating typical bone features presented at higher magnification. In a human vertebra with osteolytic bone metastasis (A), rarefication of the bone network and at higher resolution (A_1 and A_2), destruction of bone tissue (A_2: red arrow) is observed. In vertebra with osteosclerotic bone metastasis (B), higher image resolution [B_1 and B_2] shows thickening of bone trabeculae, loss of bone marrow space, and extensive trabeculae remodeling. Both processes are observed in the human vertebra with mixed bone metastases (C) and when examining regions of the cancellous bone at higher image resolution [C_1 and C_2].

Figure 2. Graphical summary of the study methodology. Fourteen metastatic human vertebral bodies (A) were mCT imaged at a resolution of 24.5mm (B) and mechanically tested (C) to measure strength and stiffness (D). Based on the mCT images, metastatic regions were identified, bone cores extracted (E), and each human bone core re-mCT was imaged at 10.5mm to evaluate the lesion's effect on bone architecture (F). The imaged cores were then processed to evaluate the lesion's effect on AGEs and collagen content (G)

Figure 3. Human osteosclerotic vertebrae show higher strength and stiffness than human osteolytic vertebrae. The strength and stiffness of human vertebrae with mixed bone metastasis appear closer to that of osteosclerotic vertebrae, suggesting the ratio bone metastasis type affects mechanical behavior. In contrast to human vertebrae with a mix or osteolytic bone metastasis, osteosclerotic human vertebrae with high strength showed high variation in stiffness.

Figure 4. Illustration of bone metastasis radiological type (osteosclerotic, n=14, Mixed, n=10 and osteolytic, n=31) effect on human cancellous bone tissue mineral content (BMC), bone volume fraction (BV/TV), and the following stereological indices [trabecular number (TbN) thickness (TbTh), separation (TbSp) and connectivity density (ConnD)] analyzed for the bone vertebral bone cores.

Figure 5 In vertebrae from doners with breast [B] and prostate [D], cancer primaries appear to affect distinct micro-architectural features in the affected cancellous bone (demonstrated by the difference in ConnD), in osteosclerotic, but not osteolytic, bone metastasis [A]. The observed pattern of bone deposition may explain this difference. High-resolution imaging of bone core obtained from breast cancer vertebra [C] exhibits a high degree of osteoid-like material in the inter-trabecular space with relatively little change in trabecular thickness. By contrast, the bone core obtained from the prostate cancer vertebra [E] exhibits remarkable, uniform thickening of the trabeculae with little or no evidence of deposition of osteoid-like material.

Figure 6. Analysis of bone tissue obtained from the bone cores revealed that bone metastases type differentially affect the association between bone volume fraction and bone mineral content and architecture. In osteolytic bone (n=31), the association of BV/TV with lower BMC, TbN, and ConnD but higher TbSp and lack of significant association for TbTh, suggests bone rarefaction via physical loss of bone tissue. In osteosclerotic bone (n=14), the association of higher BV/TV with higher BMC, TbN, TbTh but lower TbSp, and the surprising lack of association with ConnD, suggests that the sclerotic tissue may occur via thicking of trabeculae and the deposition of new osteoid-like material. Per its definition, bone with mixed bone

metastasis (n=10) showed higher BV/TV associated with BMC and TbTh, similar to osteosclerotic bone, with higher ConnD similar to osteolytic bone,

Figure 7. Analysis of human bone tissue obtained from the vertebral bone cores found bone with osteosclerotic bone metastasis contains lower AGEs and higher collagen content, indicative of higher bone remodeling, while, by comparison, the osteolytic bone higher AGEs and lower collagen content indicate lower remodeling rate and possible degradation of bone matrix.

Figure 8. tobbit regression showed higher BMC and lower AGEs values of the bone tissue associated with higher whole vertebral strength and stiffness. Note the higher variance in AGEs in the prostate bone and BMC in the breast cancer bone.

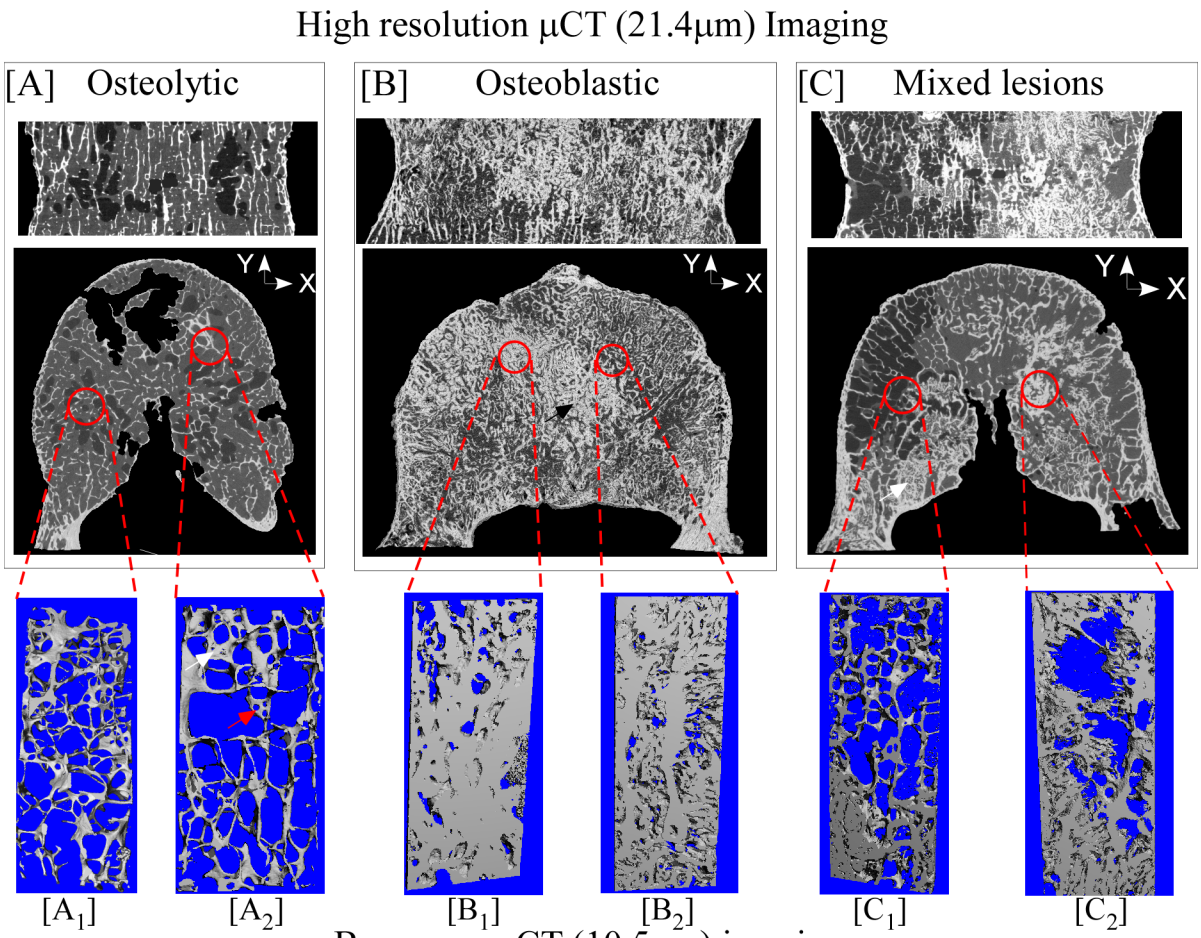

JBMR_4539_Figure 1.tif

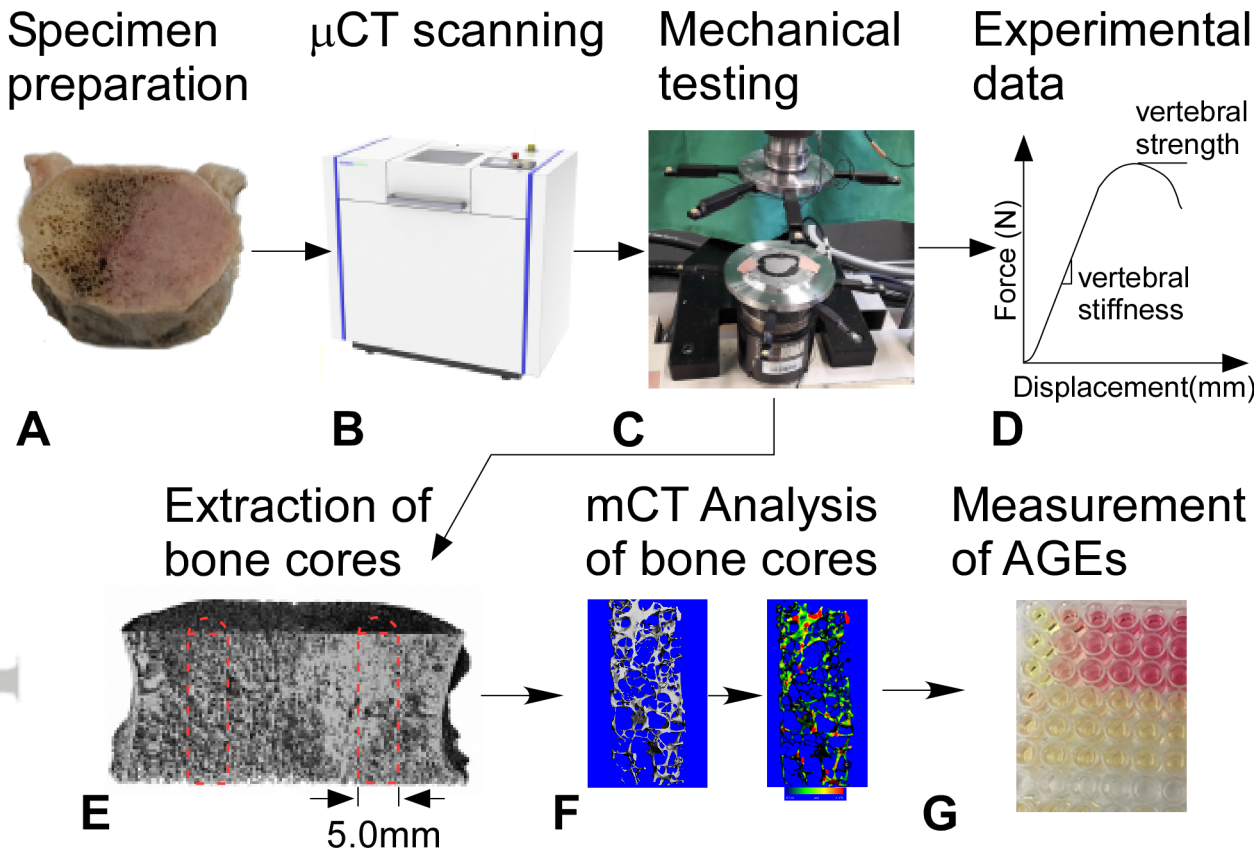

JBMR_4539_Figure 2 Graphical overview.tif

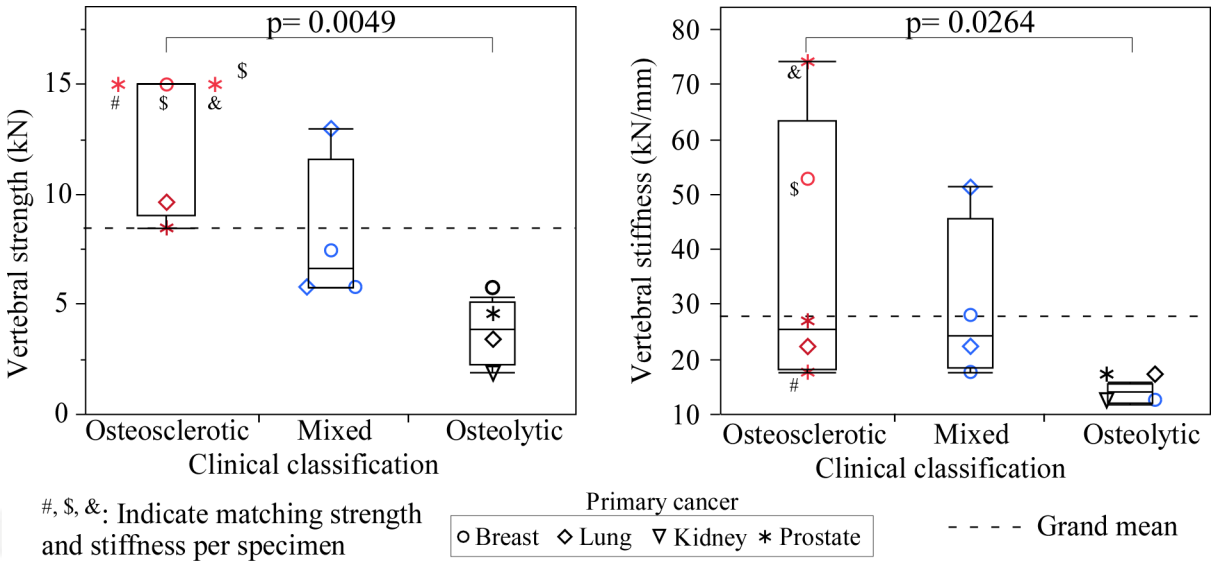

JBMR_4539_Figure 3 vertebral BM vs. strength and stiffness.tif

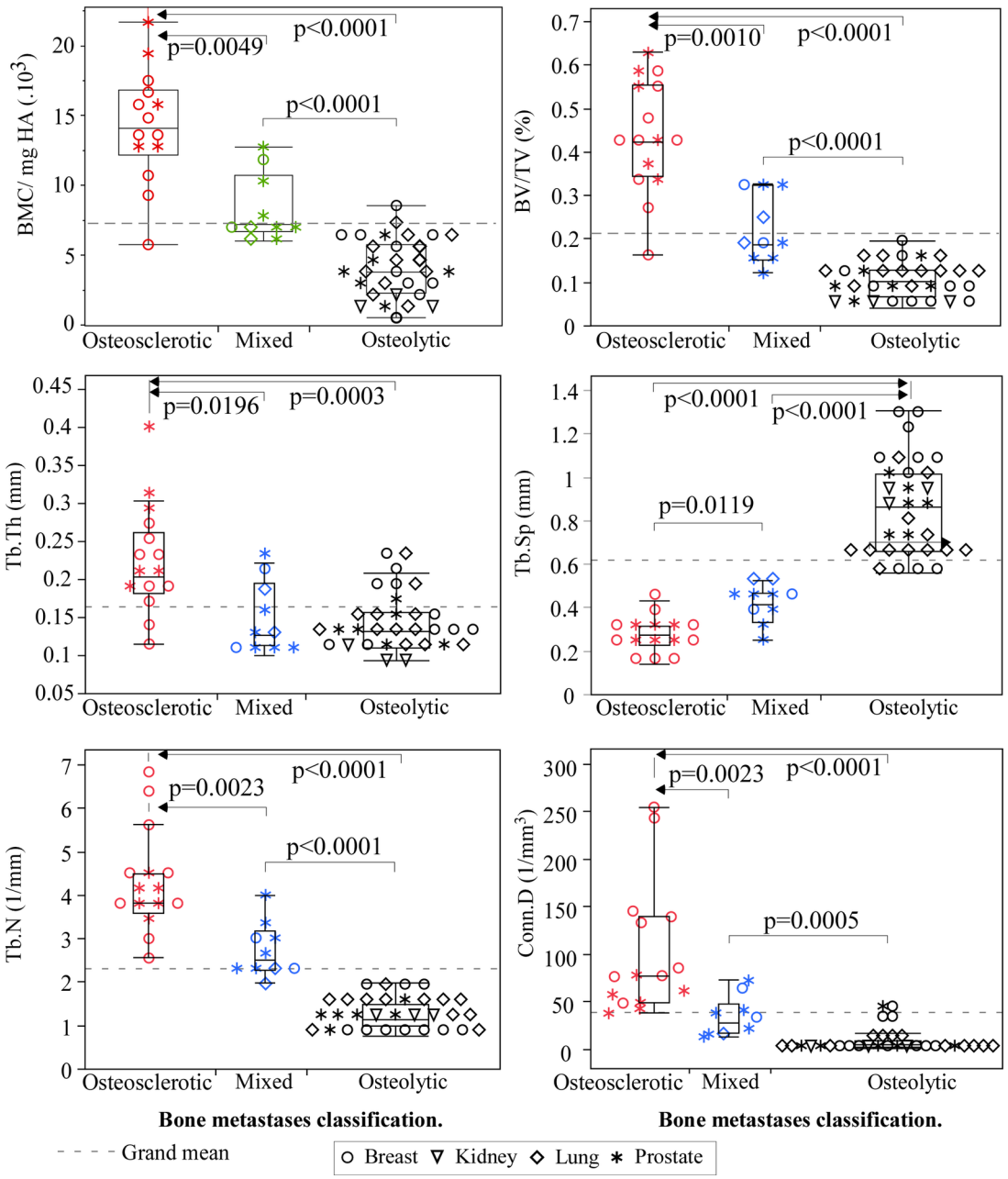

JBMR_4539_Figure 4 lesion class. vs BMC, BV-TV and architecure (box plot).tif

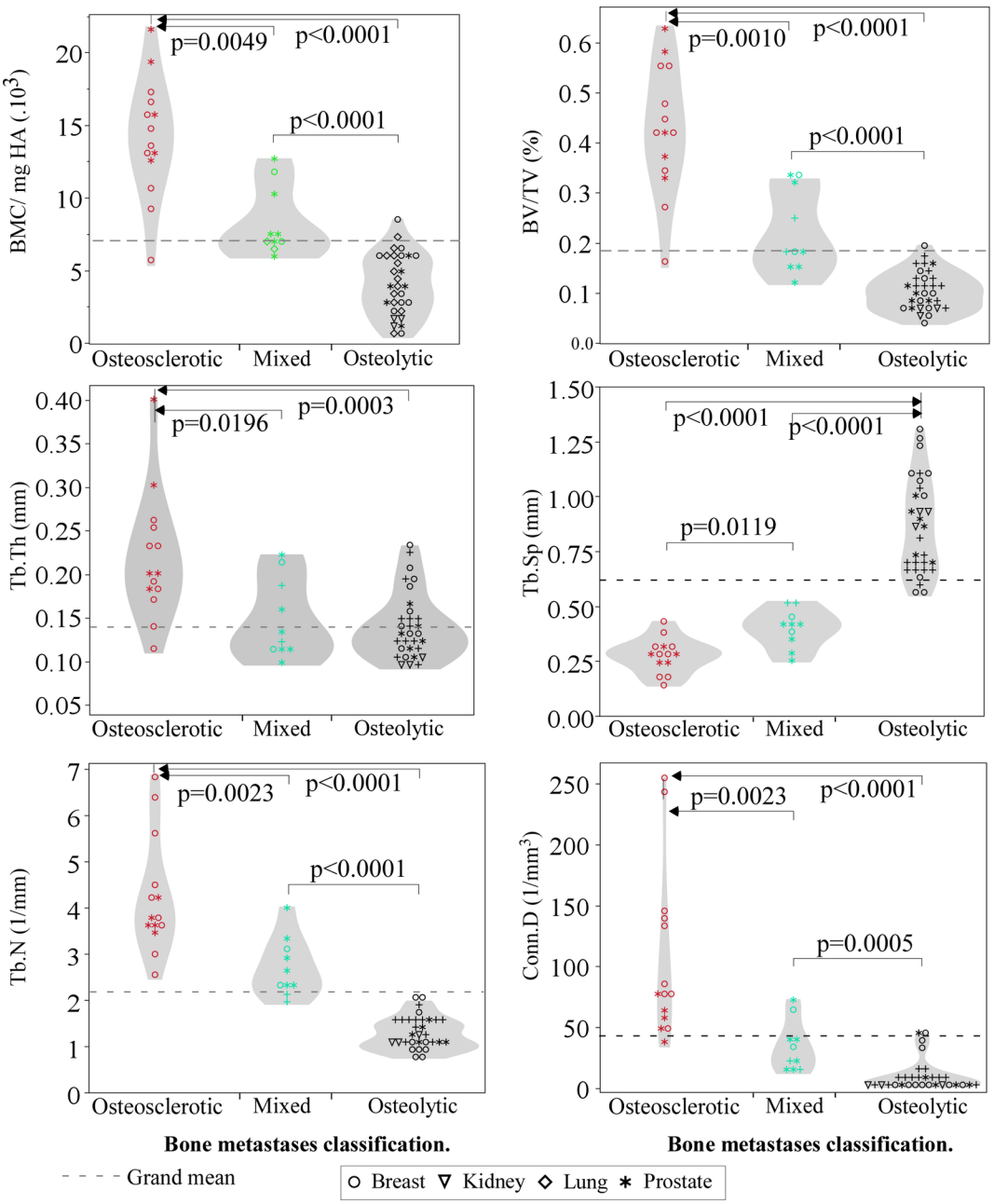

JBMR_4539_Figure 4 vertebral BM vs vBMD, BV-TV and architecure (violin plot).tif

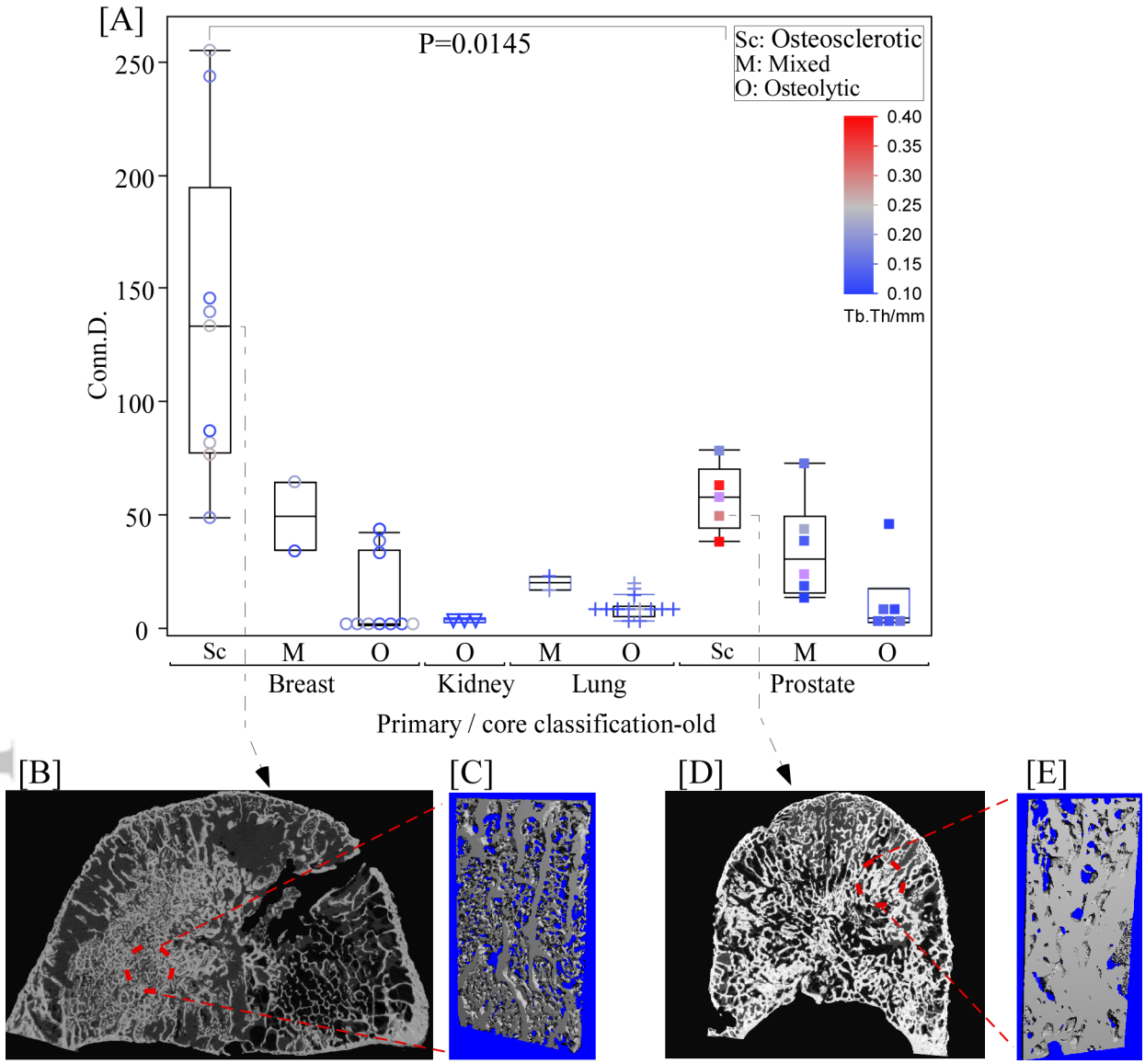

JBMR_4539_Figure 5 effect of primary on AGE and Architecture .tif

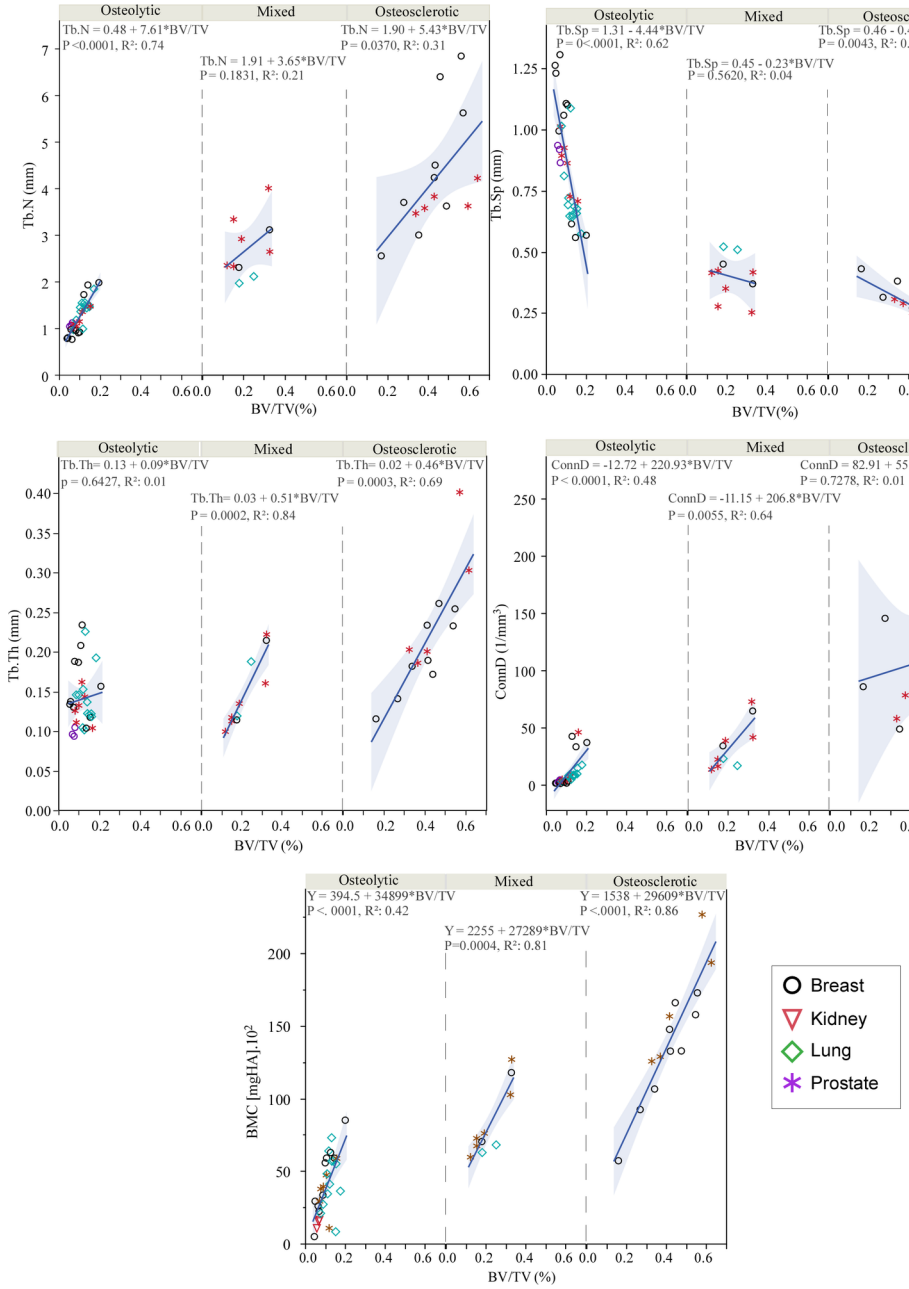

JBMR_4539_Figure-6 (revised) BV-TV vs bone arch by BM type (primary).tif

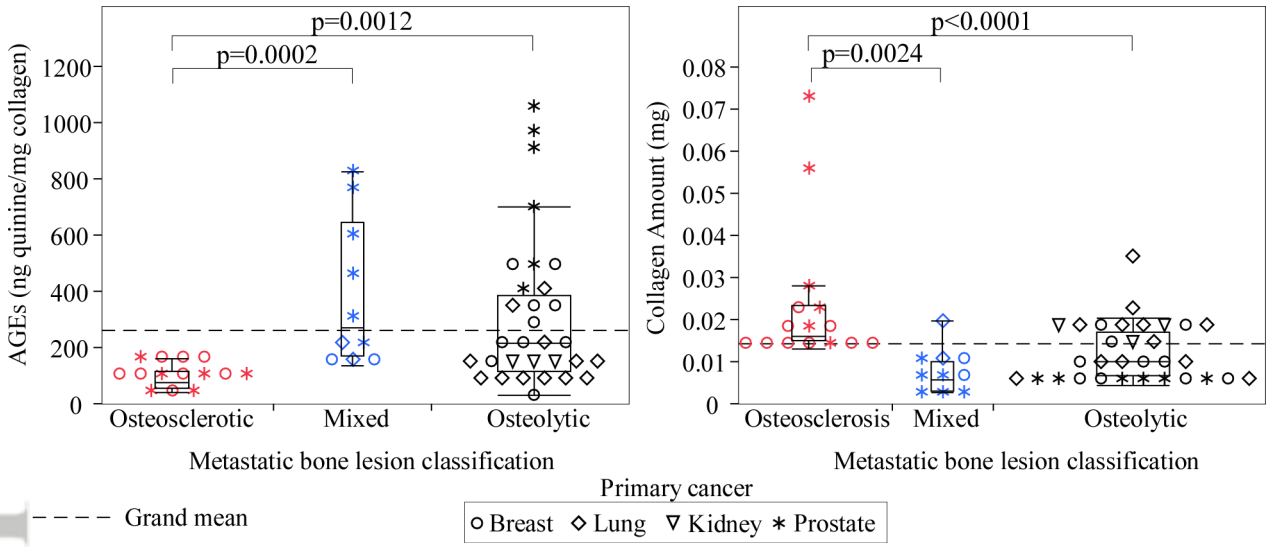

JBMR_4539_Figure 7 AGE and collagen vs lesion.tif

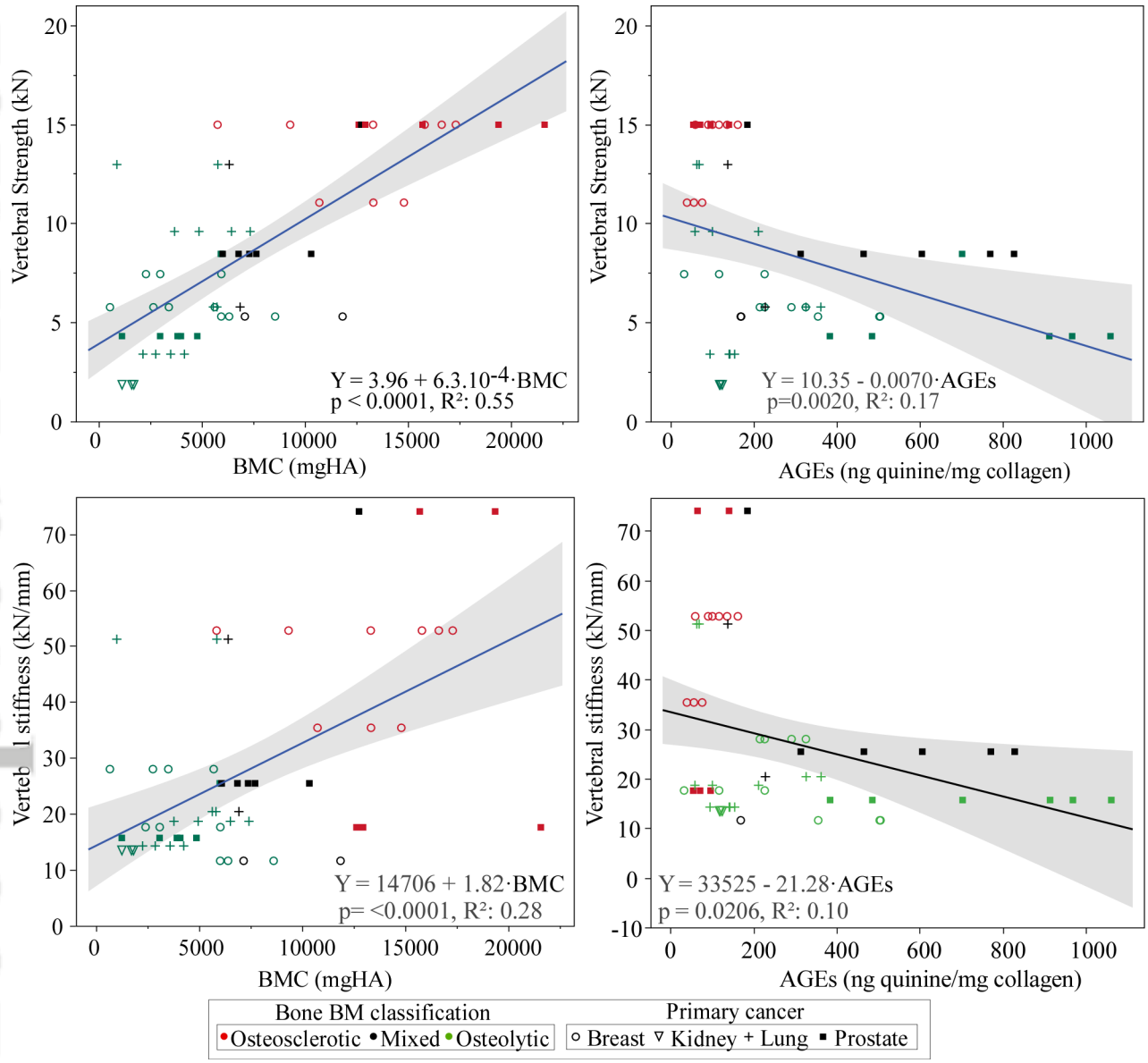

JBMR_4539_Figure-8 (revised) BMC and AGEs vs strength and stiffness.tif